NUCL SCI TECH (2020) 31:53
https://doi.org/10.1007/s41365-020-00767-w

Molecular rotation-caused autocorrelation behaviors of thermal noise in water

Yu-Wei Guo[1,2] · Jing-Yu Qin[3] · Jian-Hua Hu[4] · Ji-Hua Cao[5] · Zhi Zhu[4] · Chun-Lei Wang[6]

Received: 15 February 2020 / Revised: 16 March 2020 / Accepted: 3 April 2020 / Published online: 14 May 2020

Abstract The finite autocorrelation time of thermal noise is crucial to unidirectional transportation on the molecular scale. Therefore, it is important to understand the cause of the intrinsic picosecond autocorrelation time of thermal noise in water. In this work, we use molecular dynamics simulations to compare the autocorrelation behaviors of the thermal noise, hydrogen bonds, and molecular rotations found in water. We found that the intrinsic picosecond autocorrelation time for thermal noise is caused by finite molecular rotation relaxation, in which hydrogen bonds play the role of a bridge. Furthermore, the simulation results show that our method of calculating the autocorrelation of thermal noise, by observing the fluctuating force on an oxygen atom of water, provides additional information about molecular rotations. Our findings may advance the understanding of the anomalous dynamic nanoscale behavior of particles, and the applications of terahertz technology in measuring the structural and dynamical information of molecules in solutions.

Keywords Thermal noise · Hydrogen bond · Rotation · Molecular dynamics simulation

1 Introduction

Thermal noise, also referred to as thermal fluctuation, is ubiquitous in nature. This noise is significant in almost all physical-biochemical processes, including the movement of molecular motors [1–5], adsorption of molecules [6, 7], molecular transport [8–11], and water evaporation [12, 13]. Thermal noise plays a key role in microscopic measurements [14–16]. For example, it can be used to measure the

Yu-Wei Guo and Jing-Yu Qin have contributed equally to this work.

This work was supported by the National Key Research and Development Program of China (No. 2018YFE0205501 and 2018YFB1801500), the National Natural Science Foundation of China (No. 11904231), the Shanghai Sailing Program (No. 19YF1434100).

Electronic supplementary material The online version of this article (https://doi.org/10.1007/s41365-020-00767-w) contains supplementary material, which is available to authorized users.

✉ Zhi Zhu
zhuzhi@usst.edu.cn

✉ Chun-Lei Wang
wangchunlei@sinap.ac.cn

[1] Shanghai Institute of Applied Physics, Chinese Academy of Sciences, Shanghai 201800, China

[2] University of Chinese Academy of Sciences, Beijing 100049, China

[3] College of Education, Shanghai Normal University, Shanghai 200234, China

[4] School of Optical-Electrical Computer Engineering, University of Shanghai for Science and Technology, Shanghai 200093, China

[5] The People's Hospital of China Three Gorges University, Yichang, China

[6] Division of Interfacial Water, Shanghai Advanced Research Institute, Chinese Academy of Sciences, Shanghai 201210, China

spring constant of atomic force microscope cantilevers [17]. Furthermore, the noises associated with biological processes are important when performing single-particle tracking [18]. In traditional theories, thermal noise is modeled as Gaussian white noise with a constant power spectrum density (PSD $\sim 1/f^{\alpha}$, $\alpha = 0$) [19]. This treatment may be impractical on the nanoscale, because nanoscale phenomena typically differ from those on the macroscopic and mesoscopic scales. Gong et al. and Aluru et al. discovered the unidirectional transportation of water molecules across a water nanochannel in the presence of an asymmetric potential, in 2007 and 2008, respectively [20, 21]. In 2012, Detcheverry et al. demonstrated that the center of mass for a confined fluid performs a non-Markovian random walk in nanoporous structures, which is inconsistent with its behavior in macrosystems [22]. Initially, the existence of unidirectional transportation in nanosystems was controversial [23–25]. However, Wan et al. proved that the unidirectional transportation of molecules at the nanoscale was feasible in the presence of an appropriate asymmetric potential and a finite autocorrelation time of thermal noise [26]. They further suggested that thermal noise is crucial to unidirectional transportation in asymmetric nanosystems, and that in water it has an autocorrelation time of the order of picoseconds [26]. In other words, thermal noise in water can generate molecular driving forces in thermally fluctuating conditions. Previous theoretical and experimental studies have also shown that thermal noise cannot be treated simply as white noise on the molecular scale, it may be colored (PSD $\sim 1/f^{\alpha}$, $\alpha \neq 0$) [27–29]. In 2014, using simulations modeling different thermostat coupling methods and parameters, we discovered that the autocorrelation time of thermal noise is intrinsic. This means it depends only on the system temperature, and does not need to be evaluated through calculation, with a duration of $\sim$ 10 ps in water [27]. In 2016, we proposed (using power spectrum analysis) that the thermal noise of polar solute molecules (such as water, methanol, etc.) in water resembles a $1/f$ noise distribution (a typical non-white noise) on the nanoscale [28]. In 2019, Mukherjee et al. further confirmed that the thermal noise of protein, which is sensitive to energy fluctuations, behaves in water as $1/f$ noise [29]. Non-white thermal noise appears to be crucial to understanding the structural and dynamical characteristics of molecules or polymers in water. However, our previous work only suggested that the picosecond autocorrelation time of thermal noise may be due to the alteration of the water's hydrogen bond network [27]. Detailed research should clarify the cause of the picosecond autocorrelation time of thermal noise.

Rotation is the most basic form of molecular motion. The rotation of water molecules in the hydration layer of solutes influences various biochemical processes, including ion transport, protein folding, and chemical reactions in the solution. For example, by calculating molecular dynamics for a model $Cl^- + CH_3ClS_N2$ reaction in water, Gertner et al. observed that rotations induced the rearrangement of water molecules' hydrogen bonds and generated the conditions required for reactants to enter a transition state [30]. Bernal et al. proposed that the rotations of water molecules determine proton transport in water, and they found that the motion (including rotation) of neighboring water molecules was a key feature in the necessary solvent reorganization [31]. Our earlier research (2018) also demonstrated that limiting the rotations of the outermost water molecules can modulate the evaporation of water on a uniformly and completely wetted surface [32].

In this study, we initially employ a molecular dynamic simulation [33–39] to compare the autocorrelation behavior of thermal noise in bulk water with those of the hydrogen bonds and molecular rotations of water molecules. We discover that the molecular rotations of water molecules have an autocorrelation time of $\sim$ 10 ps, which is equal to the time of thermal noise autocorrelation in water. Moreover, the rotational autocorrelation function of water molecules closely resembles that of their thermal noise and hydrogen bonds. The variational trends in characteristic time for the autocorrelation functions of molecular rotations, hydrogen bonds, and thermal noise in water correspond to the changes in environment temperature are the same. We then study the effects of molecular rotation on the hydrogen bond network. In further simulations, we partly constrain the rotations of water molecules, by applying a uniform electric field of varying strengths. The simulation results show that restricting the rotations of water molecules can increase the lifetime of hydrogen bonds in water, indicating that molecular rotation determines the stability of the hydrogen bond network. The rotations of water molecules can alter the water's hydrogen bond network; thus, the picosecond molecular relaxation time determines the finite lifetime of hydrogen bonds in water. In addition, the intrinsic $\sim$ 10 ps autocorrelation time of thermal noise is thought to originate from alterations to the water's hydrogen bond network [27]. Therefore, the detailed cause of the picosecond autocorrelation time of thermal noise can be attributed to the finite rotation relaxation of water molecules in bulk water, where the hydrogen bonds appear to function as a bridge. Moreover, we find that our calculation method (choosing the oxygen atom of water to consider the autocorrelation characteristics of thermal noise) describes the rotational behavior information of molecules. As predicted, when the rotational freedom of the single-file water chain is restricted in a nanotube or nanopore, the thermal noise has a longer autocorrelation time and unidirectional transportation becomes significant [20, 21, 40, 41]. Finally, we analyze

the thermal noise power spectrum in a broad frequency domain for water molecules and found that thermal noise can be modeled as white noise below the terahertz frequency domain (< 0.1 THz); however, it must be regarded as non-white noise in the terahertz and higher frequency domains. The dynamic nanoscale processes usually occur on picosecond timescales (corresponding to the terahertz band). Our findings here are significant for the understanding of anomalous nanoscale behaviors, and have implications for the application of terahertz technologies in observing and detecting the structural and dynamical information of molecules in solutions.

2 Methods

As shown in Fig. 1, we placed water molecules into a simulation box (dimensions $L_X = L_Y = L_Z = 3.0$ nm) then began the simulations. All simulations were performed with a canonical ensemble using the classical molecular dynamics programming package GROMACS (version 4.5.5) [42]. The simulation system used 895 TIP3P rigid water molecules [43], because the TIP3P water model is widely used for studying the liquidity and transport properties of water. The interaction parameters of the water molecules were modeled with an OPLS/AA force field. The atomic charges of oxygen and hydrogen were −0.8476 e and 0.4238 e, respectively. The Van der Waals radius (σ_O) and well depth (ε_o) for an oxygen atom were 0.316557 nm and 0.605194 kJ/mol, respectively; the Van der Waals radius and well depth for a hydrogen atom were 0 nm and 0 kJ/mol, respectively. Under the OPLS/AA force field, the Lennard–Jones parameters between different atoms were calculated using the geometric average for $\sigma_{ij} = \left(\sigma_i\sigma_j\right)^{1/2}$ and $\varepsilon_{ij} = \left(\varepsilon_i\varepsilon_j\right)^{1/2}$; thus, the non-bonded interaction $E_{\mathrm{nb}} = \sum_i \sum_j \left[q_i q_j e^2/r_{ij} + 4\varepsilon_{ij}\left(\sigma_{ij}^{12}/r_{ij}^{12} - \sigma_{ij}^{6}/r_{ij}^{6}\right)\right]$. The bond length between a hydrogen and oxygen atom in a water molecule was 0.09572 nm. The bond angle of a water molecule (denoted as H–O–H) was 104.52°. Periodic boundary conditions were applied in all directions. Nosé–Hoover thermostats [44, 45] were used to maintain the system at a set of reference temperatures, which in this study were 285, 300, 315, 330, 345, and 360 K. Nosé–Hoover thermostats depend on two significant coupling parameters: the time constant for coupling τ_T and the period for coupling t_{couple}. When the Nosé–Hoover temperature-coupling method is applied, the equations of motion $\frac{d^2 r_i}{dt^2} = \frac{F_i}{m_i}$ for a particle are replaced by $\frac{d^2 r_i}{dt^2} = \frac{F_i}{m_i} - \zeta\frac{dr_i}{dt}$. Here, r_i is the coordinate of the i-th atom, F_i is the force exerted on the i-th atom, and m_i denotes the mass of the i-th atom. The heat-bath parameter ζ can be expressed as $\frac{d\zeta}{dt} = \frac{4\pi^2}{\tau_T^2 T_0}(T - T_0)$, where τ_T is the coupling time constant, which determines the relaxation time with which the system changes from the instantaneous temperature T to the reference temperature T_0. The coupling period t_{couple} is the time interval between two applications of the temperature-coupling method. Under the Nosé–Hoover approach, these two coupling parameters cause an oscillatory relaxation in the system, resulting in a correct canonical ensemble. The particle mesh Ewald [46] integration was used to treat the long-range electrostatic interactions. The simulation time for each system was set as 20 ns with a time step of 2 fs. The trajectory was measured every 0.2 ps (simulation results using different recording-time resolutions can be found in the ESI†), and data from the previous 10 ns were extracted to analyze the characteristics of thermal noise.

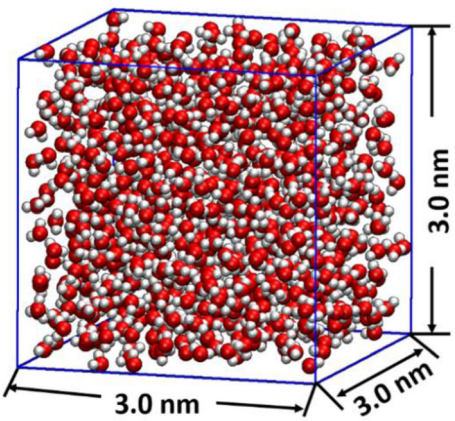

Fig. 1 (Color online) The initial simulation state with 895 TIP3P water molecules in a 3.0 × 3.0 × 3.0 nm^3 cube (simulation results with different box sizes can be seen in the ESI†). The red and gray spheres represent the oxygen and hydrogen atoms of the water molecules, respectively. The blue lines represent the boundaries of the periodic box in the simulation system

3 Results and discussion

Our simulations (Fig. 2) show that the dynamical behaviors (including the thermal noise, hydrogen bonds, and rotations) of water molecules in bulk water have an intrinsic picosecond autocorrelation time, and that the autocorrelation time of thermal noise is closely related to the autocorrelation characteristics of the hydrogen bonds and rotations of the water molecules. Typically, thermal noise, which is also referred to as thermal agitation, is caused by the random motions of particles such as electrons and ions. In molecular dynamics simulations, the thermal noise can be characterized as the randomly fluctuating force that a molecule or atom receives from its surrounding environment. Thus, we used the fluctuating

force (f) exerted on the oxygen atoms of water by surrounding water molecules to represent thermal noise in the simulations. The autocorrelation function of thermal noise is

$$C_{\text{noise}}(t) = \frac{f(0)f(t)}{f(0)f(0)}. \quad (1)$$

Here, $f(0)$ and $f(t)$ represent the forces exerted on the oxygen atom of a water molecule at times 0 and t, respectively. We first calculated the autocorrelation of thermal noise in bulk water at the reference temperature of 300 K. It can be seen from Fig. 2a that $C_{\text{noise}}(t)$ decays exponentially from 1 to 0 as the autocorrelation time t is increased. The maximum autocorrelation time (the minimum time in which $C_{\text{noise}}(t) \approx 0$) of thermal noise in bulk water was approximately 10 ps. In our previous work, we speculated that the finite correlation time of thermal noise in water was related to the dynamical behavior of the water's hydrogen bond network [27], because water molecules in bulk water maintain their tetrahedral coordination shells by forming hydrogen bonds with other water molecules in the vicinity. Hydrogen bonding is not only the main component of the interaction between a water molecule and its neighboring water molecules, it also strongly influences the physical and chemical properties of water [47–50]. Hydrogen bonds are likely to form between neighboring water molecules if the O–H bond of one molecule faces the oxygen of the next. In this study, we adopted a commonly used geometric definition of hydrogen bonding, to determine whether or not a hydrogen bond is formed. Specifically, two water molecules were considered to be hydrogen bonded if the distance between the oxygen atoms of the molecules (O···O) was less than 3.5 Å and, at the same time, the angle between the H–O bond of the water molecule and the connecting line of two oxygen atoms (H–O···O) was less than 30° [51–53]. The autocorrelation function expression of a hydrogen bond is

$$C_{\text{H-bond}}(t) = \frac{h(0)h(t)}{h(0)h(0)}, \quad (2)$$

where $h(0) = 1$ indicates that two water molecules initially form a hydrogen bond, and $h(t)$=1 indicates that the these two water molecules are still bonded at time t; otherwise, $h(t) = 0$. $C_{\text{H-bond}}(t)$ is indeed similar to $C_{\text{noise}}(t)$, resulting in a comparable autocorrelation time ($\sim$ 10 ps) (see also Fig. 2a). It is worth noting that the intrinsic dynamics of water molecules—for instance, rotations and translations—profoundly affect the lifetime of their hydrogen bonds. Thus, we further studied the autocorrelation of rotations for molecules in bulk water. A water molecule can be modeled as a set of three points, corresponding to a negatively polarized oxygen O and two positively polarized hydrogen H_1 and H_2. The angle between, and the respective lengths of, the vectors $\overrightarrow{OH_1}$ and $\overrightarrow{OH_2}$ can fluctuate. The water dipole moment vector and the vector identified from the two hydrogen atoms of each water molecule are considered

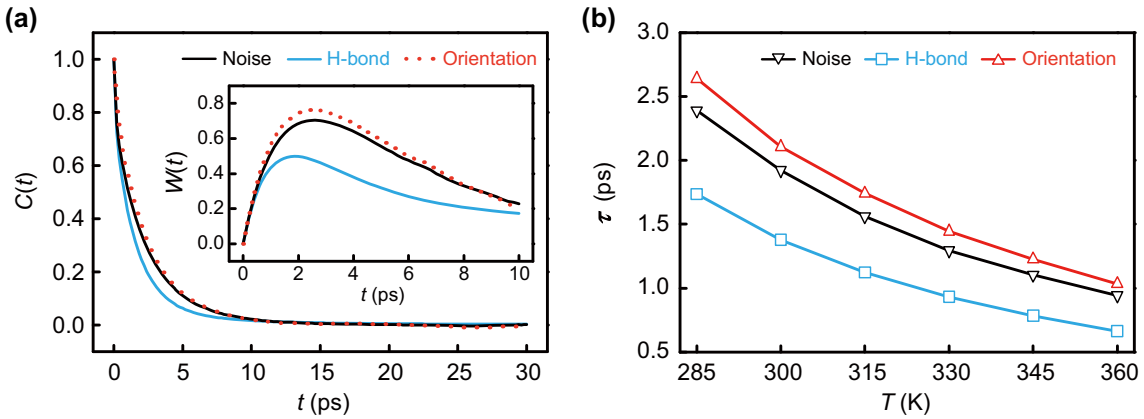

Fig. 2 (Color online) **a** The autocorrelation functions $C(t)$ for different quantities of water molecules in bulk water. The solid black, solid blue, and dotted red curves represent the autocorrelation functions of the thermal noise ($C_{\text{noise}}(t)$), hydrogen bonds ($C_{\text{H-bond}}(t)$), and molecular rotations ($C_{\text{orientation}}(t)$) of water molecules in bulk water, respectively. The inset displays the function using the expression of $W(t) = t \cdot C(t)$, in which the autocorrelation time t (with respect to the maximum value of $W(t)$) is the characteristic time of the autocorrelation function. The solid black, solid blue, and dotted red curves represent the functions for the thermal noise, hydrogen bonds, and molecular rotations, respectively. **b** The characteristic time of the autocorrelation function with different temperatures (T), which were fitted using the autocorrelation function described by a single exponential function $y = e^{\frac{-t}{\tau}}$. The solid black, blue, and red curves represent the characteristic times of the thermal noise τ_{noise}, hydrogen bonds $\tau_{\text{H-bond}}$ (also referred to as the lifetime of the hydrogen bond), and water molecular rotation τ_{rotation} in water at different temperatures, respectively. The error bars of characteristic times for thermal noise, hydrogen bonds, and molecular rotations (with respect to the temperature (285 K $\leq T \leq$ 360 K)) did not exceed 0.02 ps

here. Such molecular orientations can be conveniently described with a choice of vectors, defined as $\vec{d} = \frac{\overrightarrow{OH_1}+\overrightarrow{OH_2}}{\left|\overrightarrow{OH_1}+\overrightarrow{OH_2}\right|}$. Likewise, the autocorrelation function of molecular orientation is

$$C_{\text{orientation}}(t) = \frac{d(0)d(t)}{d(0)d(0)}, \quad (3)$$

where $d(0)$ and $d(t)$ are the dipoles of tagged water molecules at times 0 and t, respectively. As shown in Fig. 2a, it can be seen that the autocorrelation function of thermal noise for water molecules is almost identical with that of water's molecular orientation. To facilitate a quantitative comparison, we used the single exponential functions $y(t) = e^{\frac{-t}{\tau_{\text{noise}}}}$, $y(t) = e^{\frac{-t}{\tau_{\text{H-bond}}}}$, and $y(t) = e^{\frac{-t}{\tau_{\text{orientation}}}}$ to fit the autocorrelation functions of the thermal noise, the hydrogen bonds, and the orientations of the water molecules, respectively. Here, τ_{noise} is the characteristic time of the thermal noise autocorrelation,$\tau_{\text{H-bond}}$ is the characteristic time of the water hydrogen bond autocorrelation (also referred to as the lifetime of the hydrogen bond), and $\tau_{\text{orientation}}$ is the characteristic time of the molecular orientation autocorrelation. The values were 1.90, 1.38, and 2.10 ps for the τ_{noise}, $\tau_{\text{H-bond}}$, and $\tau_{\text{orientation}}$ of water molecules in bulk water at 300 K, respectively. It is worth noting that the characteristic time of hydrogen bond autocorrelation was smaller than that of thermal noise or water molecule rotation; this was a result of the hydrogen bond definition (i.e., the O–O distance $\leq$ 3.5 Å and hydrogen bond angle $\leq 30°$) [51–53]. Because the interaction between a hydrogen donor and oxygen acceptor remains after breaking of the hydrogen bond, the average lifetime of the hydrogen bond should be smaller than the characteristic time for thermal noise or water molecule rotation. Furthermore, we used $W(t) = t \cdot C(t)$ to model the characteristic time τ, because $W(t)$ has a maximum when $t = \tau$. The inset of Fig. 2a illustrates that the value of t (with respect to the maximum positions of $W(t)$) for the thermal noise, hydrogen bonds, and water orientations are almost identical, which further confirms that their respective characteristic times are also almost identical.

The thermal kinetic behavior of molecules is determined by temperature, because the reference temperature of the system determines the velocity distribution of the water molecules undergoing Brownian motion. Molecular velocity affects the collisions between the water molecules and their neighbors. At a certain temperature, the duration of the interaction between neighboring molecules is intrinsic. Therefore, the thermal noise correlation time of water molecules may also depend on the temperature, if it is also intrinsic. Thus, we proceeded to study the effect of bulk water temperature on the characteristic times of the thermal noise τ_{noise}, the hydrogen bonds $\tau_{\text{H-bond}}$, and the molecular rotations τ_{rotation}. It can be seen from Fig. 2b that τ_{noise} decreases significantly under an increase in temperature, which confirms that the autocorrelation time of thermal noise in bulk water depends on the environment temperature. Interestingly, τ_{rotation} and $\tau_{\text{H-bond}}$ also decrease as the temperature increases. This phenomenon may be attributable to fact that an increase in the reference temperature can accelerate the molecular rotational velocity of water, which causes the finite relaxation time of molecular rotation to decease. Meanwhile, the molecular rotation can affect the neighboring hydrogen bond network; thus, the hydrogen bond lifetime should decrease as the temperature increases. Notably, the changing trends of τ_{noise} and τ_{rotation} with respect to temperature are highly consistent. These facts indicate that the cause of the intrinsic picosecond autocorrelation time of thermal noise in water is the finite molecular rotation relaxation, in which the hydrogen bonds act as a bridge.

The hydrogen bond is the bridge between molecular rotation and thermal noise, which suggests that limiting the molecular rotation will prolong the dynamic adjustment time of the hydrogen bond network. To study the effects of molecular rotation on the alteration of the neighboring hydrogen bond network, we partly constrain the rotations of water molecules by applying a uniform electric field. Thus, we conducted several molecular dynamics simulations with an electric field intensity of 1, 2, 3, 4, and 5 V/nm. As shown in Fig. 3, the value of $\tau_{\text{H-bond}}$ is 1.38 ± 0.01 ps in the absence of an external electric field (i.e., E = 0 V/nm). In contrast, the lifetime of the hydrogen bonds in water increases with the electric field increase, its value is 1.39 ± 0.02 ps, 1.43 ± 0.02 ps, 1.48 ± 0.02 ps, 1.61 ± 0.02 ps, and 1.78 ± 0.03 ps for E = 1, 2, 3, 4, and 5 V/nm in the presence of an external electric field, respectively. This confirms that the lifetime of a hydrogen bond increases with the constraint strength under an increase of molecular rotation. Because the water molecule dipole is constrained by the electric field, the molecular rotation relaxation time increases as the constraint strength of molecular rotation increases. Combined with the fact that the intrinsic picosecond autocorrelation time of thermal noise stems directly from the alteration of the hydrogen bond network [27], we can conclude that the origin of the intrinsic picosecond autocorrelation time of thermal noise is the finite relaxation time of molecular rotations in water.

To confirm the relationship between the water molecule rotations and the thermal noise further, we analyzed the dynamic trajectories of water molecules in bulk water and calculated the angle θ between the molecular dipole and thermal noise vectors. Figure 4a shows the angle between the thermal noise and water molecule dipole vectors with

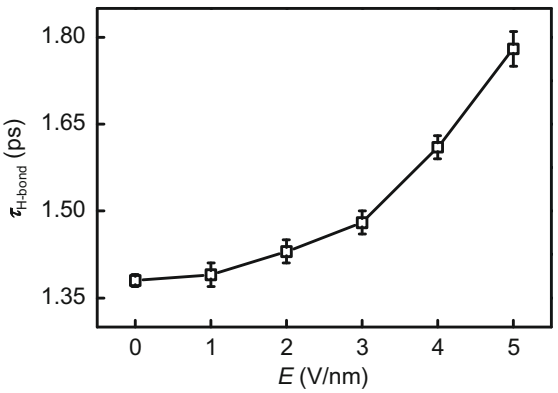

Fig. 3 The black squares with error bars represent the lifetimes of hydrogen bonds formed by water molecules in bulk water when applying different uniform electric fields to partly constrain the molecular rotation

respect to the simulation time t, where we rotated the water dipole vector in a clockwise direction until it aligned with the thermal noise vector. The angle can thus be changed from 0° to 360°. From the statistics of the time-dependent angle in Fig. 4a, we found that the angle θ between the molecular dipole vector and the noise vector predominantly fluctuated around 180°, as indicated by the red line in Fig. 4a. Our subsequent calculations (Fig. 4b), based on the probability distribution of the angle θ between the molecular dipole and noise vectors, show two peaks located at 156.9° and 213.1°. This implies that the orientation of thermal noise is almost identical with that of the molecular dipole. In our previous work [27], we speculated that the intrinsic picosecond autocorrelation time of thermal noise in water is directly derivable from the hydrogen bond network alteration. Moreover, the molecular rotation of water can induce the generation and fracture of hydrogen bonds and the water dipole vector is aligned with the thermal noise vector. These facts further confirm that the thermal noise of water molecules depends on the water molecule's rotations.

Thermal noise is a vector, which implies that the autocorrelation of thermal noise contains magnitude and direction information. Because the autocorrelation function is normalized, the magnitude of autocorrelation is averaged, thus the orientation plays a crucial role. However, the thermal noise vector is aligned with that of molecular rotation, which entails that the thermal noise and water dipole have near-identical autocorrelation functions. This means that our method of computing the fluctuating force on oxygen atoms in water [26–28] contains information pertaining to the water's dynamical behavior. Specifically, it characterizes the autocorrelation behavior of the water dipole. It is worth noting that molecules are treated as spherical particles in the traditional theory of Brownian motion; thus, the traditional theory only treats the randomly fluctuating force (that of the surrounding environment on the particle) as thermal noise. As a result, it can only represent translational information of the dynamical molecular behavior. However, the structure of a molecule is directly related to its rotation, and the rotations of the molecule directly affect its dynamic properties. Therefore, molecules cannot be simply treated as spherical particles on the nanoscale, and considering the rotations of molecules can better explain the dynamical behavior of molecules at these scales.

In traditional theory, the thermal fluctuation (thermal noise) is treated or modeled as white noise. White noise is a specific type of noise that describes a random signal or process whose autocorrelation time is zero and whose power spectral density is constant. We have detailed the cause of the intrinsic thermal noise autocorrelation time in bulk water and know that it is on the picosecond scale,

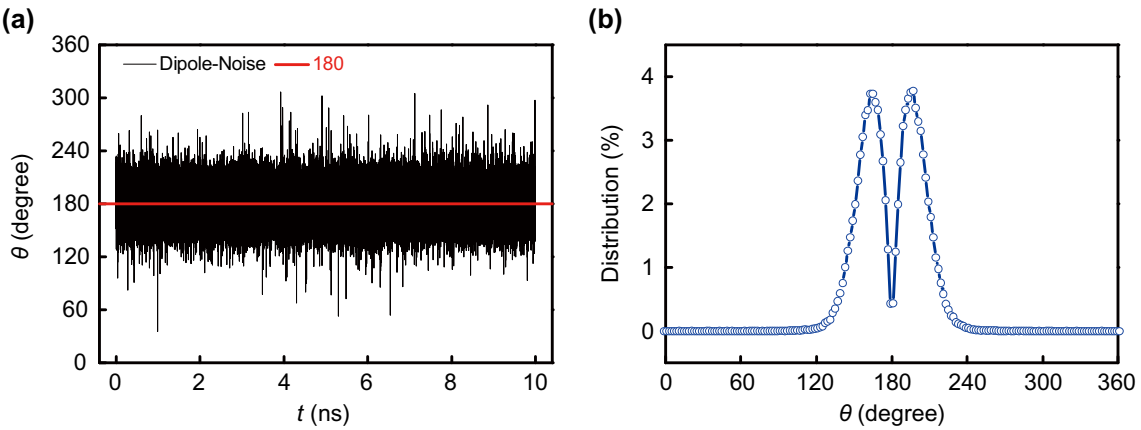

Fig. 4 The change and distribution of the angle θ between the molecular dipole and noise vectors, in the clockwise direction; here, we used the molecular dipole as the initial vector. **a** The angle θ between the molecular dipole and noise vectors with respect to the simulation time t. The dashed gray lines represent the upper and lower limits of error for the value of the time-dependent angles. **b** The probability distribution of the angle θ between the molecular dipole and noise vectors. Angles are measured in degrees

indicating that thermal noise is not white noise on the nanoscale. Here, we further study the non-white behavior of thermal noise. The power spectrum function is widely used to analyze fluctuation properties in a random process [54]; it describes the distribution of noise power with respect to frequency, and with this we can indicate the periodicities that dominate the whole process of fluctuation and distinguish the colors of the noise [55–57]. The spectral power of stationary stochastic processes is the Fourier transform of the autocorrelation function. Because the autocorrelation function of thermal noise $C_{\text{noise}}(t)$ is time-reversible (in other words, $C_{\text{noise}}(t)$ is an even function), the power spectrum of thermal noise can be expressed as

$$S(\omega) = \frac{1}{t_{\text{m}}}\int_{-tm}^{tm} C_{\text{noise}}(t)\mathrm{e}^{-i\omega t}\mathrm{d}t = \frac{2}{t_{\text{m}}}\int_{0}^{tm} C_{\text{noise}}(t)\cos(\omega t)\mathrm{d}t. \quad (4)$$

Here, t_{m} is the maximum time considered for $C_{\text{noise}}(t)$, which was here set as 1 ns. Figure 5a shows the autocorrelation function of thermal noise in water, the thermal noise autocorrelation time is $\sim$ 10 ps. We used the exponential function $R(t) = \mathrm{e}^{-t/1.90}$ to fit the autocorrelation function of thermal noise. It can further be seen from Fig. 5a that $R(t)$ fits the autocorrelation function of thermal noise well, which means that the characteristic time of thermal noise is 1.90 ps. Figure 5b shows the spectral density of the thermal noise power spectrum, which was derived from the data in Fig. 5a using Eq. (4). The spectral density is constant when the frequency ω is less than 1×10^{11} Hz, it then decreases as frequency increases from 1×10^{11} to 2.5×10^{12} Hz. Because the Fourier transform of $y(t) = \mathrm{e}^{-at}$ is $S(\omega) = \frac{2a}{a^2+\omega^2}$, $S(\omega)$ should describe the power spectrum of thermal noise well. From Fig. 5b, it can be seen that the spectral power of thermal noise indeed approximates to the function of $S(\omega) = \frac{2a}{a^2+\omega^2}$, where $a = \frac{1}{\tau_{\text{noise}}} = 5.26 \times 10^{11}$ with the frequency domain ω ranging from 1×10^{9} to 2.5×10^{12} Hz (see the inset of Fig. 5b for the spectral density of thermal noise in a wider frequency range, obtained from $S(\omega) = \frac{2a}{a^2+\omega^2}$). According to the expression for $S(\omega)$, we know that $S(\omega)$ approximates to a constant of $2/a$ when $\omega < 0.1$ THz, because ω is considerably smaller than a in this range. When $\omega > 0.1$ THz, ω is comparable to a, and $S(\omega)$ is no longer constant. This suggests that thermal noise in bulk water takes the form of white noise in the lower frequency domain and non-white noise at terahertz and higher frequency domains (see the ESI† for further discussion). Because the particle dynamics we observed on macroscopic or mesoscopic scales are low frequency, it may be feasible to treat the thermal noise as white noise on these scales. This treatment may not be appropriate at the nanoscale, because the energy of a nanoscale system is expressed by several $k_{\text{B}}T$ ranges (k_{B} represents the Boltzmann constant); thus, the magnitude of the thermal fluctuations is comparable to the thermodynamic quantities to which the system is subjected. The molecular or atomic collisions occur within a timescale of picoseconds or faster; this corresponds to high-frequency dynamics. Consequently, thermal noise is non-white at nanoscales. Thus, the biased motion of particles resulting from thermal noise may be possible in nanoscale systems if (a) spatial inversion asymmetry holds [58] and (b) we can prevent distorted measurement in high time-resolution experimental techniques by distinguishing the noise color [18].

4 Conclusion

We used molecular dynamic simulations to investigate the relationship between the autocorrelation behaviors of thermal noise, hydrogen bonds, and the molecular rotations of water molecules in bulk water. The simulation results showed that the thermal noise autocorrelation function of water molecules in bulk water is very similar to the autocorrelation functions of the hydrogen bonds and molecular rotations of water molecules. Moreover, the characteristic autocorrelation times of the thermal noise, hydrogen bonds, and water rotations exhibited the same behaviors under changes in environment temperature. Further study on the thermal noise power spectrum of water molecules shows that thermal noise on the nanoscale cannot be regarded as white noise. We found that the cause of the intrinsic picosecond autocorrelation time for thermal noise is the finite (picosecond) molecular rotation relaxation in water. The underlying mechanism arises because the rotation of water molecules induces the alteration of their hydrogen bond network, indicating that the finite molecular rotation relaxation is the origin of the finite autocorrelation time of hydrogen bonds in water. Meanwhile, the thermal fluctuating force occurs from the alteration of the hydrogen bond network in water [27], meaning the hydrogen bond plays the role of a bridge. Moreover, we found that the orientation of the molecular dipole is nearly opposite that of the thermal fluctuating force exerted on the oxygen atom of the water molecule. This result indicates that our calculation method for the thermal noise, that of choosing the oxygen atom of the water molecule to consider the autocorrelation time of thermal noise in water, provides additional information about the molecular rotation behavior.

The finite water molecular rotation relaxation time causes the finite autocorrelation time of thermal noise in water. Therefore, the thermal noise under confined conditions (such as a water channel of nanometer size) might have a longer autocorrelation time when the rotational

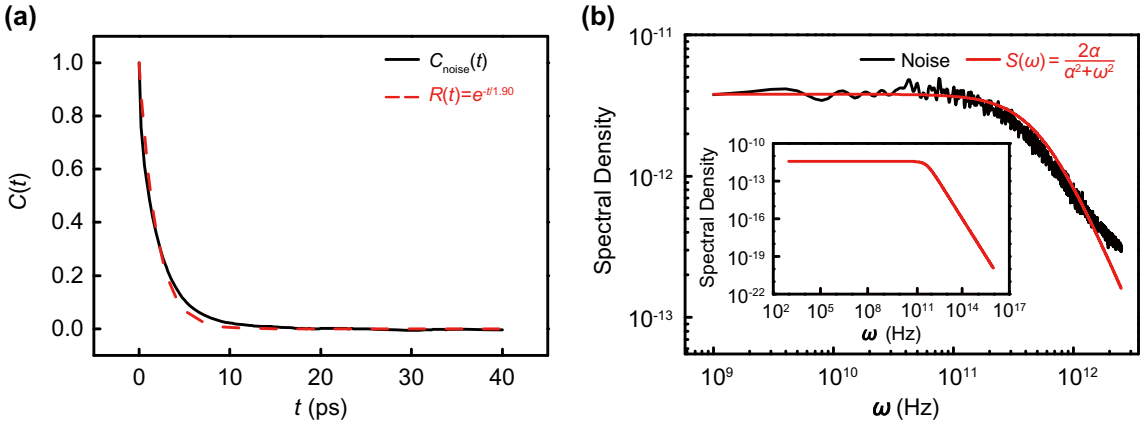

Fig. 5 (Color online) The autocorrelation function of thermal noise in the time and frequency domains, respectively. **a** The solid black curve represents the autocorrelation function of thermal noise within time t from 0 ps to 40 ps. The dashed red curve represents the fitting function $R(t) = e^{\frac{-t}{\tau_{noise}}}$ of the thermal noise autocorrelation function, where τ_{noise} = 1.90 ps is the characteristic time of thermal noise. **b** The solid black curve represents the spectral density of thermal noise in bulk water with respect to the frequency ω, which was calculated from the thermal noise autocorrelation function within the frequency domain from 1×10^9 to 2.5×10^{12} Hz. The red curve is the fitting function of $S(\omega) = \frac{2a}{a^2+\omega^2}$, where $a = \frac{1}{1.90 \times 10^{-12}} = 5.26 \times 10^{11}$; the inset illustrates the fitting function of $S(\omega)$ with a wider frequency domain (from 1×10^3 to 1×10^{16} Hz)

freedom is restricted. Therefore, the unique dynamical behavior of a single-file water chain confined in a nanotube or other porous material of similar size, in the presence of an appropriate asymmetric potential, may be made more understandable [20, 21]. It should also be noted that many physical and biochemical processes occur on the picosecond timescale, and that this timescale corresponds to the terahertz [58] frequency domain. Accordingly, our findings are expected to further understanding by using terahertz technology to observe and detect the unique physical and biochemical processes occurring on the nanoscale, and to promote the applications of terahertz technology in biomedical science.

Acknowledgements We thank Prof. Hai-Ping Fang for his constructive suggestions and are grateful to Xing Liu, Xue-Chuan Nie, Gang Fang, and Yi-Zhou Yang for their help. The authors also appreciate the support received from the Shanghai Supercomputer Center of China, the Computer Network Information Center of the Chinese Academy of Science, the National Supercomputing Center in Shenzhen (Shenzhen Cloud Computing Center), and the Special Program for Applied Research on Super Computation of the NSFC-Guangdong Joint Fund (second phase).

References

1. A. Efremov, Z. Wang, Universal optimal working cycles of molecular motors. Phys. Chem. Chem. Phys. **13**, 6223–6233 (2011). https://doi.org/10.1039/C0CP02118K
2. M. Alvarez-Pérez, S.M. Goldup, D.A. Leigh et al., A chemically-driven molecular information ratchet. J. Am. Chem. Soc. **130**, 1836–1838 (2008). https://doi.org/10.1021/ja7102394
3. A. Yildiz, P.R. Selvin, Fluorescence imaging with one nanometer accuracy: application to molecular motors. Acc. Chem. Res. **38**, 574–582 (2005). https://doi.org/10.1021/ar040136s
4. T.E. Kelly, R.A. Silva, H.D. Silva et al., A rationally designed prototype of a molecular motor. J. Am. Chem. Soc. **122**, 6935–6949 (2000). https://doi.org/10.1021/ja001048f
5. B. Wand, L. Vuković, P. Král, Nanoscale rotary motors driven by electron tunneling. Phys. Rev. Lett. **101**, 186808 (2008). https://doi.org/10.1103/PhysRevLett.101.186808
6. J. Liu, G. Shi, P. Guo et al., Blockage of water flow in carbon nanotubes by ions due to interactions between cations and aromatic rings. Phys. Rev. Lett. **115**, 164502 (2015). https://doi.org/10.1103/PhysRevLett.115.164502
7. F. Ganazzoli, G. Raffaini, Computer simulation of polypeptideadsorption on model biomaterials. Phys. Chem. Chem. Phys. **7**, 3651–3663 (2005). https://doi.org/10.1039/B506813D
8. J. Su, K. Yang, H. Guo, Asymmetric transport of water molecules through a hydrophobic conical channel. RSC Adv. **4**, 40193–40198 (2014). https://doi.org/10.1039/C4RA07034H
9. E.R. Cruz-Chu, A. Aksimentiev, K. Schulten, Ionic current rectification through silica nanopores. J. Phys. Chem. C **113**, 1850–1862 (2009). https://doi.org/10.1021/jp804724p
10. Y. Wand, Y. Zhao, J. Huang, Giant pumping of single-file water molecules in a carbon nanotube. J. Phys. Chem. B **115**, 13275–13279 (2011). https://doi.org/10.1021/jp2069557
11. C. Zhu, H. Li, S. Meng, Transport behavior of water molecules through two-dimensional nanopores. J. Chem. Phys. **141**, 18C528 (2014). https://doi.org/10.1063/1.4898075
12. X. Nan, Y.W. Guo, R.Z. Wan, Effect of Na and Cl ions on water evaporation on graphene oxide. Nucl. Sci. Tech. **30**, 122 (2019). https://doi.org/10.1007/s41365-019-0646-7
13. C. Caleman, D. van der Spoel, Evaporation from water clusters containing singly charged ions. Phys. Chem. Chem. Phys. **9**, 5105–5111 (2007). https://doi.org/10.1039/B706243E
14. R. Levy, M. Maaloum, Measuring the spring constant of atomic force microscope cantilevers: thermal fluctuations and other methods. Nanotechmology **13**, 33 (2002). https://doi.org/10.1088/0957-4484/13/1/307
15. A. Burtzlaff, A. Weismann, M. Brandbyge et al., Shot noise as a probe of spin-polarized transport through single atoms. Phys.

Rev. Lett. **114**, 016602 (2015). https://doi.org/10.1103/PhysRevLett.114.016602
16. Y. Hovav, I. Kaminker, D. Shimon et al., The electron depolarization during dynamic nuclear polarization: measurements and simulations. Phys. Chem. Chem. Phys. **17**, 226–244 (2015). https://doi.org/10.1039/C4CP03825H
17. H.J. Butt, M. Jaschke, Calculation of thermal noise in atomic force microscopy. Nanotechmology **6**, 1 (1995). https://doi.org/10.1088/0957-4484/6/1/001
18. J. Siódmiak, P. Beldowski, Hyaluronic acid dynamics and its interaction with synovial fluid components as a source of the color noise. Fluct. Noise Lett. **18**, 1940013 (2019). https://doi.org/10.1142/S0219477519400133
19. P. Hanggi, P. Jung, Colored noise in dynamical systems. Adv. Chem. Phys. **89**, 239–326 (1995). https://doi.org/10.1002/9780470141489.ch4
20. X.J. Gong, J.Y. Li, H.J. Lu et al., A charge-driven molecular water pump. Nat. Nanotechnol. **2**, 709–712 (2007). https://doi.org/10.1038/nnano.2007.320
21. S. Joseph, N.R. Aluru, Pumping of confined water in carbon nanotubes by rotation–translation coupling. Phys. Rev. Lett. **101**, 064502 (2008). https://doi.org/10.1103/PhysRevLett.101.064502
22. F. Detcheverry, L. Bocquet, Thermal fluctuations in nanofluidic transport. Phys. Rev. Lett. **109**, 024501 (2012). https://doi.org/10.1103/PhysRevLett.109.024501
23. D.J. Bonthuis, K. Falk, C.N. Kaplan et al., Comment on "pumping of confined water in carbon nanotubes by rotation–translation coupling". Phys. Rev. Lett. **105**, 209401 (2010). https://doi.org/10.1103/PhysRevLett.105.209401
24. D.J. Bonthuis, D. Horinek, L. Bocquet et al., Electrokinetics at aqueous interfaces without mobile charges. Langmuir **26**, 12614–12625 (2010). https://doi.org/10.1021/la9034535
25. M.E. Suk, N.R. Aluru, Suk and Aluru Reply. Phys. Rev. Lett. **105**, 209402 (2010). https://doi.org/10.1103/PhysRevLett.105.209402
26. R.Z. Wan, J. Hu, H.P. Fang, Asymmetric transportation induced by thermal noise at the nanoscale. Sci. China Phys. Mech. **55**, 751–756 (2012). https://doi.org/10.1007/s11433-012-4695-8
27. Z. Zhu, N. Sheng, R.Z. Wan et al., Intrinsic autocorrelation time of picoseconds for thermal noise in water. J. Phys. Chem. A **118**, 8936–8941 (2014). https://doi.org/10.1021/jp5009785
28. Z. Zhu, N. Sheng, H.P. Fang et al., Colored spectrum characteristics of thermal noise on the molecular scale. Phys. Chem. Chem. Phys. **18**, 30189–30195 (2016). https://doi.org/10.1039/C6CP04433F
29. S. Mukherjee, S. Mondal, B. Bagchi, Mechanism of solvent control of protein dynamics. Phys. Rev. Lett. **122**, 058101 (2019). https://doi.org/10.1103/PhysRevLett.122.058101
30. B.J. Gertner, R.M. Whitnell, K.R. Wilson et al., Activation to the transition state: reactant and solvent energy flow for a model SN2 reaction in water. J. Am. Chem. Soc. **113**, 74–87 (1991). https://doi.org/10.1021/ja00001a014
31. J.D. Bernal, R.H. Fowler, A theory of water and ionic solution, with particular reference to hydrogen and hydroxyl ions. J. Chem. Phys. **1**, 515–548 (1933). https://doi.org/10.1063/1.1749327
32. Y.W. Guo, R.Z. Wan, Evaporation of nanoscale water on a uniformly complete wetting surface at different temperatures. Phys. Chem. Chem. Phys. **20**, 12272–12277 (2018). https://doi.org/10.1039/C8CP00037A
33. C.N. Peng, The effects of hydrogen on the helium behavior in palladium. Nucl. Sci. Tech. **27**, 106 (2016). https://doi.org/10.1007/s41365-016-0115-5
34. W. Xu, Y.S. Tu, C.L. Wang et al., Water transport through T-shaped carbon nanotubes. Nucl. Sci. Tech. **22**, 307–310 (2011). https://doi.org/10.13538/j.1001-8042/nst.22.307-310
35. X. Ren, B. Zhou, C. Wang, Promoting effect of ethanol on dewetting transition in the confined region of melittin tetramer. Nucl. Sci. Tech. **23**, 252–256 (2012). https://doi.org/10.13538/j.1001-8042/nst.23.252-256
36. L.W. Gao, X.B. Xia, X.Q. Xu et al., Immobilization of radioactive fluoride waste in aluminophosphate glass: a molecular dynamics simulation. Nucl. Sci. Tech. **29**, 92 (2018). https://doi.org/10.1007/s41365-018-0443-8
37. X.C. Nie, B. Zhou, C.L. Wang et al., Wetting behaviors of methanol, ethanol, and propanol on hydroxylated SiO_2 substrate. Nucl. Sci. Tech. **29**, 18 (2018). https://doi.org/10.1007/s41365-018-0364-6
38. C.L. Zhao, W.Z. Sun, X.D. Lv et al., Incident angle effect on F^+ ions interaction with β-SiC: Molecular dynamics simulation. Nucl. Tech. **34**, 1 (2011). http://d.old.wanfangdata.com.cn/Periodical/hjs201101012. **(in Chinese)**
39. Y.F. Ding, Z.B. Zhang, X.Z. Ke et al., Investigation on single carbon atom transporting through the single-walled carbon nanotube by MD simulation. Nucl. Tech. **28**, 4 (2005). https://doi.org/10.3321/j.issn:0253-3219.2005.04.012. **(in Chinese)**
40. N. Sheng, Y.S. Tu, P. Guo et al., Asymmetrical free diffusion with orientation-dependence of molecules in finite timescales. Sci. China Phys. Mech. **56**, 1047–1052 (2013). https://doi.org/10.1007/s11433-013-5081-x
41. J.Y. Su, H.X. Guo, Control of unidirectional transport of single-file water molecules through carbon nanotubes in an electric field. ACS Nano **5**, 351–359 (2011). https://doi.org/10.1021/nn1014616
42. S. Pronk, S. Pall, R. Schulz et al., GROMACS 4.5: a high-throughput and highly parallel open source molecular simulation toolkit. Bioinformatics **29**, 845–854 (2013). https://doi.org/10.1093/bioinformatics/btt055
43. W.L. Jorgensen, J. Chandrasekhar, J.D. Madura et al., Comparison of simple potential functions for simulating liquid water. J. Chem. Phys. **79**, 926–935 (1983). https://doi.org/10.1063/1.445869
44. S. Nose, A molecular dynamics method for simulations in the canonical ensemble. Mol. Phys. **52**, 255–268 (1984). https://doi.org/10.1080/00268978400101201
45. W.G. Hoover, Canonical dynamics: equilibrium phase-space distributions. Phys. Rev. A **31**, 1695–1697 (1985). https://doi.org/10.1103/PhysRevA.31.1695
46. T. Darden, D. York, L. Pedersen, Particle mesh Ewald: an N·log(N) method for Ewald sums in large systems. J. Chem. Phys. **98**, 10089–10092 (1993). https://doi.org/10.1063/1.464397
47. W. Nadler, T. Krausche, Universality in hydrogen-bond networks. Phys. Rev. A **44**, 7888–7890 (1991). https://doi.org/10.1103/PhysRevA.44.R7888
48. L.J. Zhang, W. Jian, L. Yi et al., A novel water layer structure inside nanobubbles at room temperature. Nucl. Sci. Tech. **25**, 060503 (2014). https://doi.org/10.13538/j.1001-8042/nst.25.060503
49. M.X. He, M. Li, Z. Tian et al., Terahertz spectral properties of melamine and its deuterated isotope, melamine-d_6. Nucl. Sci. Tech. **23**, 209–214 (2012). https://doi.org/10.13538/j.1001-8042/nst.23.209-214
50. S.J. Shao, P. Guo, L. Zhao et al., Ordered water monolayer on ionic model substrates studied by molecular dynamics simulations. Nucl. Sci. Tech. **25**, 020502 (2014). https://doi.org/10.13538/j.1001-8042/nst.25.020502
51. Z. Zhu, H.K. Guo, X.K. Jiang et al., Reversible hydrophobicity–hydrophilicity transition modulated by surface curvature. J. Phys. Chem. Lett. **9**, 2346–2352 (2018). https://doi.org/10.1021/acs.jpclett.8b00749
52. Z. Zhu, C. Chang, Y.S. Shu et al., Transition to a superpermeation phase of confined water induced by a terahertz

electromagnetic wave. J. Phys. Chem. Lett. **11**, 256–262 (2019). https://doi.org/10.1021/acs.jpclett.9b03228
53. G. Hummer, J.C. Rasaiah, J.P. Noworyta, Water conduction through the hydrophobic channel of a carbon nanotube. Nature **414**, 188–190 (2001). https://doi.org/10.1038/35102535
54. M. Thomas, M. Brehm, R. Fligg et al., Computing vibrational spectra from ab initio molecular dynamics. Phys. Chem. Chem. Phys. **15**, 6608–6622 (2013). https://doi.org/10.1039/C3CP44302G
55. D.L. Gilden, Cognitive emissions of 1/f noise. Psychol. Rev. **108**, 33–56 (2001). https://doi.org/10.1037/0033-295X.108.1.33
56. P. Stoica, R.L. Moses, *Spectral Analysis of Signals* (Pearson Prentice Hall, Upper Saddle River, 2005)
57. D.L. Gilman, T. Thornton, M.W. Mallon, 1/f noise in human cognition. Science **267**, 1837–1839 (1995). https://doi.org/10.1126/science.7892611
58. T. Ji, H.W. Zhao, P.Y. Han et al., Terahertz identification and quantification of penicillamine enantiomers. Nucl. Sci. Tech. **24**, 010201 (2013). https://doi.org/10.13538/j.1001-8042/nst.2013.01.005